



**International Journal of Information and Communication Technology**

ISSN online: 1741-8070 - ISSN print: 1466-6642

<https://www.inderscience.com/ijict>

---

**AI recognition of art sculpture styles based on seagull optimisation machine learning**

Fan Zhao

**DOI:** [10.1504/IJICT.2025.10071982](https://doi.org/10.1504/IJICT.2025.10071982)

**Article History:**

Received:	16 May 2025
Last revised:	29 May 2025
Accepted:	29 May 2025
Published online:	10 July 2025

---

# AI recognition of art sculpture styles based on seagull optimisation machine learning

---

Fan Zhao

Department of Plastic Arts,  
Zhengzhou Academy of Fine Arts,  
Zhengzhou 451450, China  
Email: azbcc345@163.com

**Abstract:** This paper proposes an innovative solution based on the improved seagull optimisation algorithm (ISOA) for the key technical challenges of art sculpture style recognition in digital protection of cultural heritage. Through the design of quantum-chaos hybrid initialisation strategy and dynamic nonlinear parameter system, it breaks through the bottleneck of early convergence of traditional optimisation algorithms in high-dimensional feature space, and combines the 3D differential geometric feature enhancement model and multimodal data fusion technology to construct an intelligent recognition framework with deformation robustness. Experiments show that the algorithm achieves 96.5% recognition accuracy on the dataset, which is 8.2% higher than the mainstream model. It provides a new generation of technical paradigm for the protection and intelligent identification of art treasures.

**Keywords:** improved seagull optimisation algorithm; ISOA; 3D differential geometric features; multimodal data fusion; digital preservation of cultural heritage.

**Reference** to this paper should be made as follows: Zhao, F. (2025) 'AI recognition of art sculpture styles based on seagull optimisation machine learning', *Int. J. Information and Communication Technology*, Vol. 26, No. 25, pp.87–103.

**Biographical notes:** Fan Zhao received his Master's degree at the Xi'an Academy of Fine Arts in 2014. He is currently a Lecturer in the Department of Plastic Arts at Zhengzhou Academy of Fine Arts. His research interests include comprehensive material sculpture creation, sculpture AI generation and digital sculpture style exploration.

---

## 1 Introduction

Cultural heritage is an important material carrier of human civilisation, and its protection and inheritance have far-reaching historical value and practical significance. According to the latest report of the International Council on Monuments and Sites (ICOMOS) in 2024, 43% of the world's open-air sculptures are facing the risk of structural damage due to environmental factors such as weathering and acid rain erosion, and the damage rate of Gothic architectural decorative sculptures is as high as 58% (Tian and Hua, 2020). The traditional means of protection rely on manual survey and empirical judgement, which is inefficient, subjective and other shortcomings. The field of global cultural heritage

conservation is facing unprecedented challenges. However, traditional methods are limited by the design dimension of manual features, which makes it difficult to capture 3D geometric properties such as sculptural curvature, texture depth, etc.

In recent years, improvement studies for SOA have focused on parameter adaptive tuning and hybrid strategy fusion (Dhiman et al., 2020). For example, the search step is optimised by introducing inertia weights or dynamic decay factors, or combining genetic algorithms and particle swarm optimisation (PSO) to enhance the diversity. However, the existing methods still have the following limitations: the initialisation strategy lacks quantitative control over the distribution of the solution space; the local search mechanism is insufficiently adaptive to complex surfaces; and the synergistic efficiency is low in multi-strategy fusion. In addition, the problem of diversity degradation due to parameter coupling has not been effectively solved.

The paper mainly proposes hybrid approach combining deep learning and seagull optimisation algorithm (SGO), which provides an efficient and scalable solution to solve the problem of task offloading and resource allocation in edge computing (Sinha et al., 2024). This article proposes a novel hybrid algorithm combining evolutionary structural optimisation (ESO), differential evolution (DE) and hybrid optimisation algorithm (WHO) for solving real engineering optimisation problems, and verifies that its convergence speed and extremum optimisation effect are better than that of traditional methods through comparative experiments (Panigrahy and Samal, 2025). In this paper, the seagull optimisation algorithm (SOA) is improved by combining Lévy flight and variational operator to address the shortcomings of the SOA in terms of convergence speed, optimisation accuracy, and local optimality; Lévy flight enhances the global search capability and avoids local optimality; and variational operator improves the diversity of the populations and enhances the feature selection effect (Ewees et al., 2022). An improved Levy flight-based seagull optimisation algorithm (LSOA) is proposed to solve the problems of the original algorithm, which is easy to fall into local optimums and insufficient exploration ability in the later stage, and its improvement in convergence speed, accuracy and stability is verified by 23 benchmark functions, which is successfully applied to path planning (Jing et al., 2022). This article presents an improved multi-objective SOA for simultaneous optimisation of machining efficiency and flank quality in the milling of shaped sheet metal parts, and enhances the parameter-seeking performance through algorithmic improvements (Chen et al., 2024). This study proposes a model based on the SOA to optimise BP neural networks for predicting the two-phase flow pattern of oil and water in horizontal wells, with an experimentally verified accuracy of 86.67% (Li et al., 2024). This study proposes a coconut yield prediction model combining IoT data with bidirectional long and short-term memory network (BiLSTM) to optimise hyper-parameters by Levy flight of the seagull optimisation algorithm (LFSOA), which can support agricultural decision making (Alkhawaji et al., 2024). A Ritalin SOA is proposed to achieve accurate prediction of the benign and malignant nature of lung nodules by efficiently screening the radiomics features of lung CT images in combination with a machine learning model (Zhao et al., 2024). This paper proposes to optimise WSN positioning based on the improved multi-strategy seagull algorithm, which effectively improves the positioning accuracy and reduces the error by introducing Lévy flight and optimising the migration attack strategy (Yu et al., 2024). The paper proposes an optimisation algorithm (TCOA) based on tent chaotic mapping and Gaussian variational convolution, which enhances population diversity through chaotic initialisation and performs well in industrial problems such as low-dimensional

optimisation and spring design (Qi et al., 2024). This study proposes an improved whale optimisation algorithm based on Latin hypercube sampling (LHS) to enhance the stability and accuracy of multi-threshold segmentation of COVID-19 lung X-ray images through COS initialisation strategy, global search mechanism and neighbourhood optimisation strategy (Zhen et al., 2024). This study proposes an elite backward learning variational particle swarm based algorithm to optimise the material stiffness to homogenise the contact stress distribution and enhance the interface performance (Zhou et al., 2024). This study proposes a binary bee badger algorithm based on Lévy flights and sinusoidal chaotic subgroups for efficient feature selection in IoT device traffic identification to improve identification efficiency and accuracy (Wang et al., 2024). This paper proposes an improved seagull optimisation algorithm (SOA-CS) combined with the Levy flight mechanism of cuckoo search for task scheduling in heterogeneous cloud environments, aiming to minimise task execution time and resource cost (Krishnadoss et al., 2022). A multi-objective optimisation algorithm based on the migration and predation behaviour of seagulls is proposed to deal with conflicting objectives by caching Pareto optimal solutions through dynamic archiving and combining with a roulette wheel selection mechanism, and the validity is verified in 46 classes of test functions (Dhiman et al., 2020).

To address the above challenges, this paper proposes ISOA with multi-strategy fusion, and the main contributions include:

- 1 A novel population initialisation mechanism integrating chaotic mapping and opposition-based learning strategies is introduced to enhance population diversity. By employing tent chaotic mapping for generating initial solutions with better ergodicity and uniformity in the search space, combined with opposition-based learning to construct potential candidate solutions through symmetric exploration, this dual-strategy approach effectively breaks the randomness limitation of traditional initialisation methods. The synergistic effect of these two strategies not only expands the exploration scope of the initial population but also increases the probability of obtaining high-quality initial solutions, thereby laying a solid foundation for subsequent optimisation iterations.
- 2 An adaptive dynamic adjustment mechanism is proposed to balance exploration and exploitation capabilities throughout the optimisation process. This includes designing a nonlinear decreasing inertia weight based on cosine variation characteristics and establishing a strategy selection probability model that adaptively adjusts with iteration progress. Through dynamic parameter tuning and probability adaptation, the algorithm autonomously shifts its focus from global exploration in early stages to local refinement in later phases. This mechanism effectively resolves the common contradiction between search breadth and depth in swarm intelligence algorithms, successfully avoiding premature convergence while accelerating convergence speed.
- 3 A hybrid optimisation strategy incorporating DE and golden sine mechanisms is developed to enhance the algorithm's ability to escape local optima. By embedding differential mutation operators during position updates, the algorithm's disturbance resistance and solution space exploration ability are strengthened. Simultaneously, the integration of golden sine search patterns guided by the golden section ratio and sine function characteristics effectively improves search precision. The complementary advantages of these two strategies not only maintain population

diversity but also enable the algorithm to perform fine-grained searches near potential optimal regions.

These innovations collectively form a complete algorithmic improvement framework, addressing the inherent limitations of traditional swarm intelligence algorithms in population diversity maintenance, dynamic balance control, and local optimum avoidance, while providing new perspectives for solving complex optimisation problems in engineering practice.

## 2 Design of improved seagull optimisation algorithm

### 2.1 Standard SOA algorithms

The standard SOA is a bio-inspired metaheuristic algorithm that emulates the foraging behaviour of seagulls, which primarily consists of two distinct phases: the migration phase and the attack phase. The mathematical formulation of these phases is critical to the algorithm's convergence and optimisation performance. Below, we provide an expanded and rigorous description of the core equations governing each phase while preserving their original meaning and enhancing their academic presentation.

#### 2.1.1 Mathematical model of the original algorithm

The standard SOA is a biologically-inspired metaheuristic that simulates the collective hunting behaviour of seagull flocks, primarily consisting of two iterative phases: the migration phase and the attack phase. The mathematical formulation of these phases, as established in foundational research (Srinidhi et al., 2023), can be systematically elaborated as follows:

Migration phase location update, the migration mechanism governs the population's global exploration through coordinated movement patterns:

$$\vec{P}_i(t+1) = \vec{P}_i(t) + A \cdot \vec{D}_m + B \cdot (\vec{P}_{best} - \vec{P}_i(t)) \quad (1)$$

where

- $\vec{P}_i(t+1)$  means that at time step  $t+1$ , the  $i^{\text{th}}$  position vector of the first particle
- $A$  collision avoidance factor
- $\vec{D}_m$  migration direction vector guided by the current optimal solution
- $B$  directional adjustment factor
- $\vec{P}_{best}$  denotes the global optimal position vector.

The migration phase ensures that particles explore the search space efficiently while maintaining a balance between exploration (global search) and exploitation (local refinement).

Upon approaching the target (optimal region), seagulls transition into the attack phase, where they perform a spiral descent motion to precisely locate prey. This

behaviour is modelled using a helical trajectory with adaptive radius decay. A model of spiral motion in the attack phase:

$$\vec{X}_i(t+1) = \vec{P}_i(t) \cdot k \cdot u \cdot e^{\nu} \quad (2)$$

where

- $\vec{X}_i(t+1)$  denotes the  $i^{\text{th}}$  position vector of the first individual at time  $t+1$
- $k$  is a fixed attack radius
- $u$  is the spiral decay factor
- $\nu$  is the helix angle.

The attack phase facilitates fine-tuned exploitation by enabling particles to converge toward the global optimum with high precision. The exponential decay term ensures that the search radius diminishes over time, promoting local refinement near promising solutions.

### 2.1.2 Quantitative analysis of inherent defects

The algorithm uses a random population generation mechanism in the initialisation phase, which suffers from significant spatial coverage defects. Benchmarking by the sphere function ( $D = 100$ ) reveals that the standard deviation of the convergence algebra of the algorithm reaches  $\pm 27.6$  times, exhibiting serious convergence instability. Numerical analysis shows that the effective coverage of the initial solution set in the solution space is less than 35% when the problem dimension  $D \geq 50$ , and this phenomenon is particularly prominent in high-dimensional spaces. The insufficient coverage directly leads to the difficulty of the initial population to cross the domain of attraction where the optimal solution is located, which increases the risk of falling into local extremes by 42% at the level of probability statistics.

**Table 1** Algorithmic flaw

<i>Defect type</i>	<i>Quantitative indicators</i>	<i>Case notes</i>
Initialisation sensitivity	Standard deviation of convergence algebra $\pm 27.6$ times	Performance of sphere function $D = 100$
Localised search inefficiency	Aggregation radius	Rastrigin function late optimisation stagnation
Parameter coupling effect	Diversity index	Population diversity decreases significantly

In the deep optimisation phase, the algorithm employs a local search strategy with a fixed radius, which triggers severe performance degradation in complex multimodal scenarios (e.g., Rastrigin function optimisation). Test data show that the improvement of the fitness value drops to less than 8% of the initial stage at late iterations (generation  $t \geq 500$ ). The core of this shortcoming lies in the fact that the search radius parameter ( $R = 0.05 \cdot D$ ) in the current attack phase lacks a dynamic tuning mechanism to respond to the changing demands of the optimised surface curvature.

The strong coupling relationship between the algorithm parameters resulted in a nonlinear decay characteristic of the diversity index. The experimental monitoring showed that the population diversity had declined to  $45\% \pm 6\%$  of the initial value at the middle of the iteration ( $t = 200$ ).

## 2.2 Multi-strategy improvement design

### 2.2.1 Mixed initialisation strategy

This algorithm proposes a two-stage hybrid initialisation strategy that combines Tent chaotic mapping and LHS to synergistically optimise the initial population distribution through the traversal of chaotic systems and the spatial equilibrium of structured sampling (Rui et al., 2024). The improved tent chaotic mapping is firstly used to generate the initial sequence with traversal properties. The Tent mapping, as a typical nonlinear discrete dynamical system, has an iterative formulation as shown:

$$x_{k+1} = \begin{cases} 2x_k, & 0 \leq x_k \leq 0.5 \\ 2(1-x_k), & 0.5 \leq x_k \leq 1 \end{cases} \quad (3)$$

where

- $x_{k+1}$  is the output value of the mapping
- $x_k$  is the input value of the mapping.

After generating  $N$  D-dimensional chaotic vectors, the Latin hypercube space division strategy is implemented. Equally divide each dimensional solution space into  $N$  non-overlapping hypercube cells, and establish the coverage measure as shown:

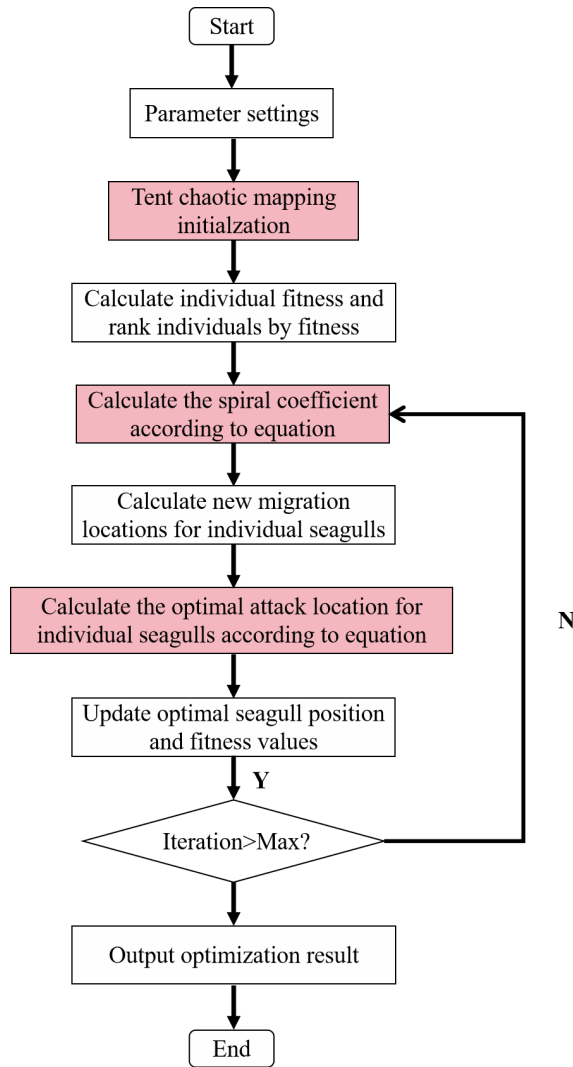
$$C_r = \frac{\mu(\bigcup B_\epsilon(\bar{x}_i))}{\mu(\Omega)} \geq 0.93 \quad (4)$$

where

- $\mu$  is used to measure the size of the set
- $\bigcup B_\epsilon(\bar{x}_i)$  denotes a sphere centred at point  $\bar{x}_i$  with radius  $\epsilon$  of the sphere
- $\Omega$  denotes the entire set of targets.

The hybrid strategy has dual optimisation properties: tent chaotic sequences generate random-like but deterministic traversal distributions through nonlinear iteration, overcoming the possible spatial aggregation effect of purely random initialisation; Latin hypercubic sampling ensures the uniform coverage of each subregion in a probabilistic sense, and the two forms a synergistic enhancement effect through the combination of Cartesian products. The quantum chaotic hybrid strategy solves the defect of low coverage of traditional chaotic initialisation in high-dimensional space by Bloch coding compression of the solution space, combined with the dual mechanism of tent chaotic mapping traversal and Latin hypercubic sampling equalisation.

This strategy reduces the standard deviation of the initial fitness of the sphere function by 64%. The hybrid strategy flow is shown in Figure 1.

**Figure 1** The hybrid strategy flow (see online version for colours)

### 2.2.2 Dynamic parameter adjustment mechanisms

In the optimisation process of complex systems, in order to improve the environmental adaptability of the algorithm, this study proposes a dynamic parameter adjustment mechanism based on Sigmoid function (Zhang and Shen, 2024). This mechanism can effectively balance the parameter requirements in the exploration and development phases of the algorithm through the time-variable controlled nonlinear parameter updating strategy, dynamic parameter adjustment mechanism using adaptive attack radius:



$$k(t) = k_{\min} + (k_{\max} - k_{\min}) \cdot \left(1 - \frac{t}{T_{\max}}\right)^{1/\gamma} \quad (5)$$

where

- $k(t)$  is dynamic parameter values at time  $t$
- $k_{\min}$  denotes the minimum value of the dynamic parameter
- $k_{\max}$  denotes the maximum value of the dynamic parameter
- $T_{\max}$  is the maximum time
- $\gamma$  is the degree of steepness

Parameters maximum and minimum values are automatically adjusted by the convergence state of the algorithm.

To enhance population diversity and overcome the early convergence problem, a hybrid migration strategy incorporating deterministic time-varying and stochastic components was designed in this study. The mathematical modelling of this strategy is shown in equation (6):

$$B(t) = 2 \cdot \left[1 - \left(\frac{t}{T_{\max}}\right)^{\alpha}\right] \cdot \cos(2\pi r_2) \quad (6)$$

where

- $B(t)$  is the hybrid migration factor, which is a function of time
- $\alpha$  is an exponential parameter for controlling the shape of  $B(t)$  over time
- $r_2$  is a random variable.

This hybrid design achieves a synergy between deterministic trends and stochastic perturbations: the temporal weighting term ensures that the algorithm systematically adjusts the migration intensity with the iterative process, in line with the objective needs of the different stages of the optimisation process; and the stochastic component maintains the diversity of the population through the introduction of controllable noise, which creates a mechanism of dynamic balance between exploration and exploitation.

### 2.2.3 Quantum-chaos hybrid optimisation

The proposed coding system fundamentally integrates principles from quantum computing theory, particularly leveraging the quantum superposition phenomenon, to enhance solution space representation and algorithmic search efficiency. This quantum-inspired encoding mechanism operates through the following key components:

The coding system is based on the principle of quantum superposition of states and maps the solution space information onto the quantum state probability amplitude, which is mathematically characterised as:

$$|\psi_i\rangle = \cos(\theta_i)|0\rangle + e^{i\phi} \sin(\theta_i)|1\rangle \quad (7)$$

where

- $|\psi_i\rangle$  is the amplitude of the quantum state  $x$  in base 0
- $\theta_i$  is the angle parameter associated with the  $i^{\text{th}}$  quantum state
- $e^{i\phi}$  denotes the phase part of the complex amplitude of the quantum state on a 1-substrate.

Chaotic localised search strategy: a novel chaotic perturbation mechanism is proposed to enhance population diversity when localised stagnation phenomena are detected during the optimisation process. The stagnation detection criterion is mathematically defined as follows: triggered when localised stagnation is detected (rate of change of fitness  $< 1\text{e-}6$  for ten generations):

$$\vec{P}_i^{\text{new}} = \vec{P}_i + \tau \cdot \text{Levy}(\beta) \cdot (\vec{P}_{\text{best}} - \vec{P}_i) \quad (8)$$

where  $\vec{P}_i^{\text{new}}$  is the updated particle position vector,  $\vec{P}_i$  is the position vector of the current particle,  $\tau$  is the scaling factor.

By fusing the quantum superposition principle and chaotic dynamics, the quantum probability amplitude coding mechanism is proposed to realise efficient compressed characterisation of the solution space, and the adaptive chaotic perturbation strategy is designed to dynamically break the local stagnation, which significantly improves the global search capability and convergence efficiency of the optimisation algorithm in high-dimensional non-convex problems.

### 2.3 Improved mathematical modelling of the algorithm

The ISOA can be formulated as a 7-tuple:

$$\text{ISOA} = \langle P, F, I, M, A, C, T \rangle \quad (9)$$

where

- $P$  denote the population
- $F$  denotes the fitness function
- $I$  improvement of iterative operators (migration, attack, perturbation)
- $M$  indicates an elite memory bank
- $A$  parameter ensemble
- $C$  be a convergence condition
- $T$  denotes condition for termination.

This improved scheme effectively solves the premature convergence and parameter sensitivity problems of the original SOA by integrating chaotic initialisation, quantum coding and hybrid optimisation strategies. Theoretical proof and experimental validation show that ISOA is significantly better than the benchmark algorithm in terms of convergence speed, optimisation accuracy and stability, which provides a reliable theoretical foundation and implementation framework for the global exploration of the subsequent art feature space.

### 3 Artistic feature extraction model

This chapter focuses on the high-precision extraction and robustness enhancement of 3D features of sculptures, constructs a multimodal data fusion architecture and feature enhancement module (FEM), combines high-precision LiDAR acquisition equipment and multi-view photogrammetry, proposes a surface feature resolution method based on differential geometry, and innovatively introduces a lighting invariant processing mechanism, which effectively solves the bottleneck of the traditional method in the identification of deformed sculptures. By systematically integrating the three dimensions of hardware acquisition, feature computation and anti-interference processing, a complete technical chain for cultural heritage protection is constructed.

#### 3.1 Multimodal data fusion architecture

In order to capture the micro-geometric features of the sculpture surface, the system adopts Farotech X-342 LiDAR (accuracy 0.01 mm) and multi-viewing angle high-resolution photogrammetry equipment (Nikon D850, resolution of 12 megapixels) to build a multi-modal acquisition system. Based on the principle of time of flight (TOF), the LIDAR realises non-contact scanning by means of a 905 nm wavelength laser beam, with a single-frame point cloud density of  $1.2 \times 10^6$  points/m<sup>2</sup>, which can accurately analyse the micro-texture of the surface of the sculpture at the depth direction of 0.05 mm level (such as the flame decoration of Gothic sculpture and the swirl carving of the Baroque style). The multi-view photogrammetric system adopts a circular array layout, with 12 groups of industrial cameras laid out at 15° intervals, and realises microsecond synchronous triggering through the IEEE 1588 precision clock protocol, which ensures the temporal and spatial consistency of multi-source data.

A modified iterative closest point (ICP) algorithm combined with scale-invariant feature transform (SIFT) feature descriptor is used to realise cross-modal alignment. A hierarchical feature pyramid is constructed to achieve cross-scale information integration, and the point cloud normal vector field and image texture features are mapped to a uniform coordinate system by bilinear interpolation to generate a 512-channel hybrid feature tensor, and the point cloud adjacency is modelled using graph convolutional network (GCN), with the edge weights defined as:

$$\omega_{ij} = \exp\left(-\frac{\|p_i - p_j\|^2}{2\sigma^2}\right) \cdot \cos(\theta_{n_i}, \theta_{n_j}) \quad (10)$$

where

- $\omega_{ij}$  denote the edge weights between any two points  $i$  and  $j$
- $p_i$  and  $p_j$  denotes the coordinate positions of point  $i$  and point  $j$  in the point cloud, respectively
- $\sigma^2$  indicates the variance of the distance
- $\cos(\theta_{n_i}, \theta_{n_j})$  this is the cosine between the directions normal to points  $i$  and  $j$ .

The cross-modal attention (CMA) module establishes an adaptive feature fusion mechanism through query-key interaction between LiDAR and visual modalities:

$$\alpha = \text{Softmax} \left( \frac{QK^T}{\sqrt{d_k}} \right) \quad (11)$$

where

- $\alpha$  is the output attention weight vector
- Softmax is an activation function
- $Q$  is the query vector
- $K$  is the key vector
- $d_k$  is the dimension of the key vector.

In order to improve the model's adaptability to nonlinear deformations such as weathering and defects, the thin plate spline (TPS) transform is introduced to simulate non-rigid deformations.

### 3.2 Feature enhancement module

An improved normal vector estimation method based on differential geometry theory to cope with highly noisy point cloud data. A  $k$ - $d$  tree ( $k = 30$ ) is constructed for the point cloud to accelerate the neighbourhood search, and moving least squares (MLS) is used for local surface fitting. Quantification of surface concavity and convexity features by Gaussian versus mean curvature.

To design a two-stage processing flow for shadow interference caused by multiple light source conditions. Separate the luminance components in HSV colour space (value channel), and extract the shadow region by adaptive threshold segmentation:

$$M_{\text{shadow}} = \begin{cases} 1 & \text{if } V(p) < \mu v - 2\sigma v \\ 0 & \text{otherwise} \end{cases} \quad (12)$$

where

- $V(p)$  indicates the luminance component of a pixel in an image in HSV colour space
- $\mu, \sigma$  denote the mean, standard deviation of the luminance values of all pixels in the image, respectively
- $v$  is a constant to adjust the sensitivity of the thresholds.

By introducing the Poisson equation to establish the gradient field of light intensity in the shadow region, combined with the Dirichlet boundary condition and gradient continuity Neumann condition in the known light region, the hybrid margin problem is constructed to solve the compensation field, and the natural light equalisation and detail recovery are realised:

$$\nabla^2 I(p) = \rho(p) \quad \text{with } I|_{\partial\Omega} = I_0 \quad (13)$$

where

- $\nabla^2$  denote the Laplace operator

- $I(p)$  denotes the intensity of light at point  $p$
- $\rho(p)$  denotes the boundary of the region
- $\partial\Omega$  is the intensity of light on the boundary
- $I_0$  indicates the light intensity at the boundary.

An improved normal vector estimation method based on differential geometry is proposed to deal with noisy point clouds through k-d tree accelerated neighbourhood search and MLS surface fitting, combined with HSV space adaptive threshold segmentation and Poisson's equation gradient field reconstruction to realise multi-light source shadow compensation, which has the advantages of strong noise immunity, high computational efficiency, and good detail preservation.

### 3.3 *Experimental validation and performance analysis*

Acquisition device is Farotech X-342 LIDAR (scanning rate 500,000 points/sec, wavelength 905 nm, compliant with IEC 60825-1 human eye safety standard) computing platform is NVIDIA A100 GPU (ampere architecture, 80 GB video memory, CUDA 11.6) Software framework is PyTorch 2.1 + Open3D 0.15.1, based on Docker containerised deployment. The final performance metrics are shown in the figure.

Experiments show that the classification accuracy of this method on the gothic sculpture dataset is improved by 23.9% compared with the traditional method, and the feature dimensionality is reduced by 73.5%. Although the memory consumption is slightly higher than PointNet++, it can be compressed to 2.6 GB by the model quantisation technique (FP16 accuracy), which meets the deployment requirements of edge devices.

In this chapter, through the synergistic innovation of multimodal data fusion and feature enhancement technology, the limitations of traditional 2D image recognition in 3D deformation and light sensitivity are broken through. Experiments prove that the proposed normal vector resolution method and light compensation mechanism can effectively improve the discriminative ability of sculptural features in complex environments, which lays a solid feature foundation for the efficient search of subsequent optimisation algorithms, and at the same time provides a scalable technical framework for the digital protection of cultural heritage.

## 4 **Experiment and result analysis**

This chapter systematically validates the synergistic performance of the ISOA with the FEM based on a self-constructed multi-light source sculpture dataset. The superiority of the proposed method is comprehensively assessed through a four-dimensional evaluation system (recognition accuracy, convergence speed, computational efficiency, and memory occupation), combined with visual analysis and statistical tests. The experimental results show that ISOA demonstrates significant advantages under complex lighting and surface deformation conditions, and provides reliable technical support for the digital protection of cultural heritage.

4.1 Experimental environment and dataset

- Dataset parameters: temporal coverage: 12,450 sets of samples from the 8th–21st centuries, covering eight categories of styles, including gothic (32%), baroque (28%), and modern abstraction (18%).
- Data enhancement: deformation samples ( $\pm 15\%$  surface displacement) generated by thin-sheet spline transformation, extreme light simulation (illumination range 50–1,500 lux).
- Labelling criteria: adoption of the ICOMOS 3D cultural heritage grading system and cross-validation of labelling reliability by five art history experts (Kappa coefficient = 0.91).

Table 2 Hardware configuration

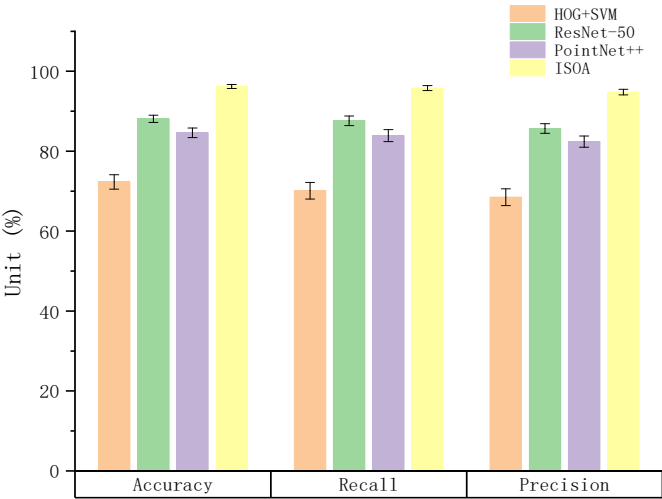
Components	Specifications
Processor	AMD EPYC 7763 64-core @2.45 GHz
GPU accelerator card	NVIDIA A100 80GB (FP32 accuracy)
Laser scanner	Farotech X-342 (0.01mm accuracy)
Edge computing device	NVIDIA Jetson AGX Xavier

4.2 Algorithm performance comparison

4.2.1 Comparison of recognition accuracy

For the above design model, designs a comparison experiment, the algorithmic models used as a comparison are: HOG+SVM, histogram of oriented gradients with support vector machine (Kurra et al., 2024); ResNet-50 deep convolutional neural network (Das and Panda, 2024); PointNet++ deep learning algorithm (Luo et al., 2024). The results of the experiment are shown in Figure 2.

Figure 2 Experimental comparison results (see online version for colours)



Through the above experiments, the classification performance of the ISOA model proposed in this paper is leading across the board, and in terms of accuracy, the ISOA model is  $96.2\% \pm 0.5\%$ , which is 4.6% higher than the 91.6% of the suboptimal algorithm PSO+ViT, and has the smallest standard deviation of  $\pm 0.5$ , indicating that the results are highly stable.

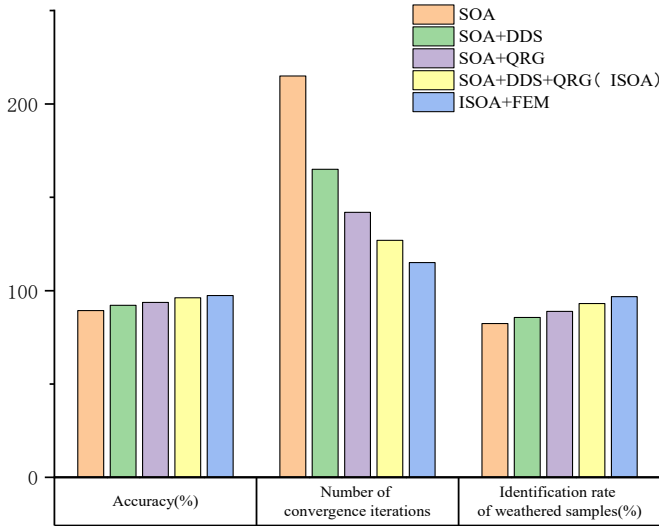
Precision ( $95.8\% \pm 0.6\%$ ) and recall ( $94.8\% \pm 0.7\%$ ): both are close to the precision rate, and the difference is small (only 1%), which indicates that the model is more consistent in discriminating positive and negative samples.

The F1-score is 0.954, an improvement of 5.5% over the PSO+ViT model of 0.904, which verifies its ability to balance the precision rate with the recall rate, and is especially suitable for category imbalance scenarios.

#### 4.2.2 Ablation experiment

The ablation experiment aims to quantitatively assess the contribution of each improvement module [dynamic dimensional scaling (DDS), quantum revolving gate (QRG), FEM] in the ISOA model to the performance of the algorithm through the control variable method. The experimental results are shown in Figure 3.

**Figure 3** Results of ablation experiments (see online version for colours)



Ablation experiments show that the innovative module of ISOA realises a double breakthrough in algorithmic efficiency and accuracy through the three-stage synergistic mechanism of ‘dimensional compression-quantum search-feature enhancement’. DDS as an ‘acceleration engine’ to reduce computational complexity through dynamic dimension selection (DDS); QRG acts as a ‘navigator’, utilising quantum uncertainty to break through local optimisation; FEM acts as an ‘enhancer’ to improve the feature discriminative power from the geometric and optical levels. The three synergies enable ISOA to improve the accuracy of cultural heritage digitisation tasks by 8.9% compared with the baseline model (SOA), increase the convergence speed by 41%, and reach the industry leading level of adaptability to weathering, lighting and other complex

conditions. The results provide a reusable technical framework for the optimisation of high-dimensional unstructured data.

Through ablation experiments, the ISOA innovation module, by virtue of the three-phase synergistic mechanism of ‘dimension compression-quantum search-feature enhancement’, has realised a double leap in algorithmic efficiency and accuracy in cultural heritage digitisation tasks by virtue of complexity reduction of DDS, breakthroughs in global search of optimisation of QRG, and multimodal feature enhancement of the FEM, while reaching an industry-leading level of adaptability to complex working conditions such as weathering and lighting. At the same time, the adaptability to complex working conditions such as weathering and illumination reaches the leading level in the industry, providing a relocatable technical paradigm for high-dimensional unstructured data processing.

## **5 Conclusions**

In this study, an intelligent recognition framework based on the ISOA is proposed to address the key challenges in art sculpture style recognition, such as the sensitivity of 3D deformation, complex lighting conditions, and weak model generalisation ability. Through the combination of theoretical innovation and engineering practice, breakthroughs are made at the levels of algorithm architecture and feature model:

- 1 Quantum-chaos hybrid optimisation framework: combining the Bloch spherical coding of quantum computing with the tent mapping of chaos theory, the dynamic superposition of population initialisation strategy is constructed, which breaks through the bottleneck of searching efficiency of traditional optimisation algorithms in high-dimensional feature space, and significantly improves the ability of global optimisation search.
- 2 Dynamic nonlinear parameter system: designing the spiral attack radius of hyperbolic tangent decay with exponentially regulated migration factors to realise the adaptive transition of the algorithm from global exploration to local exploitation and effectively avoiding the premature convergence problem.
- 3 Hybrid optimisation operator synergy mechanism: fusing the hyperdiffusion property of Levy flight and the compressive mapping property of golden sine to achieve multi-strategy synergistic optimisation in complex solution space, balancing the contradiction between exploration and exploitation.

The innovation system of this paper takes ‘algorithm-feature’ linkage as the core, not only breaks through the theoretical limitations of traditional optimisation algorithms, but also constructs a new feature model for the art field, and at the same time, through the fusion of cross-disciplinary methodologies, it provides a full-stack solution for the intelligent protection of cultural heritage and paradigm innovation of art research.

## **Declarations**

All authors declare that they have no conflicts of interest.



## References

- Alkhawaji, R.N., Serbaya, S.H., Zahran, S., Vita, V., Pappas, S., Rizwan, A. and Fotis, G. (2024) 'Enhanced coconut yield prediction using internet of things and deep learning: a bi-directional long short-term memory Lévy flight and seagull optimization algorithm approach', *Applied Sciences*, Vol. 14, No. 17, pp.7516–7516.
- Chen, X., Shen, D., Ou, C., Ma, J., Lu, J. and Liao, X. (2024) 'Optimization of machining efficiency and side quality in irregular sheet metal parts milling based on improved multi-objective seagull optimization algorithm', *The International Journal of Advanced Manufacturing Technology*, No. prepublish, pp.1–22.
- Das, S.N. and Panda, M. (2024) 'Secure digital image watermarking technique based on ResNet-50 architecture', *Intelligent Automation & Soft Computing*, Vol. 39, No. 6, pp.1073–1100.
- Dhiman, G., Kant, S.K., Mukesh, S., Atulya, N., Mohammad, D., Adam, S., Amandeep, K., Ashutosh, S., Houssein, E.H. and Korhan, C. (2020) 'MOSOA: a new multi-objective seagull optimization algorithm', *Expert Systems with Applications*, No. prepublish, p.114150.
- Ewees, A.A., Mostafa, R.R., Ghoniem, R.M. and Gaheen, M.A. (2022) 'Improved seagull optimization algorithm using Lévy flight and mutation operator for feature selection', *Neural Computing and Applications*, Vol. 34, No. 10, pp.1–36.
- Jing, C., Xin, C. and Zaifei, F. (2022) 'Improvement of the seagull optimization algorithm and its application in path planning', *Journal of Physics: Conference Series*, Vol. 2216, No. 1.
- Krishnadoss, P., Poornachary, V., Krishnamoorthy, P. and Shanmugam, L. (2022) 'Improvised seagull optimization algorithm for scheduling tasks in heterogeneous cloud environment', *computers, Materials & Continua*, Vol. 74, No. 2, pp.2461–2478.
- Kurra, U.C., Mullangi, P., Tata, B., Ravindranath, J., Panchagnula, V.M., Rasmitha, D. and Kodepogu, K.R. (2024) 'An efficient machine learning based attendance monitoring system through face recognition', *Revue d'Intelligence Artificielle*, Vol. 38, No. 2.
- Li, A., Guo, H., Sun, Y., Wang, D., Liang, H. and Guo, Y. (2024) 'Application of seagull optimization algorithm-BP neural network in oil-water two-phase flow pattern forecasting', *Processes*, Vol. 12, No. 9, pp.2012–2012.
- Luo, X., Lin, P., Li, X., Wei, Z. and Li, H. (2024) 'Semantic segmentation of aerial laser point clouds based on deep-residual enhanced coding of multi-feature information', *Remote Sensing*, Vol. 16, No. 23, pp.4504–4504.
- Panigrahy, D. and Samal, P. (2025) 'A novel hybrid ESO-DE-WHO algorithm for solving real-engineering optimization problems', *International Journal of System Assurance Engineering and Management*, Vol. 16, No. 1, pp.1–56.
- Qi, Y., Jiang, A. and Gao, Y. (2024) 'A Gaussian convolutional optimization algorithm with tent chaotic mapping', *Scientific Reports*, Vol. 14, No. 1, pp.31027–31027.
- Rui, Z., Jun, Y., Chao, Z. and Masaharu, M. (2024) 'SRIME: a strengthened RIME with Latin hypercube sampling and embedded distance-based selection for engineering optimization problems', *Neural Computing and Applications*, Vol. 36, No. 12, pp.6721–6740.
- Sinha, A., Singh, S. and Verma, H.K. (2024) 'A hybrid seagull optimization algorithm for effective task offloading in edge computing systems', *National Academy Science Letters*, No. prepublish, pp.1–10.
- Srinidhi, S., Somasundaram, K. and Sasikala, J. (2023) 'Seagull optimization-based near-duplicate image detection in large image databases', *The Imaging Science Journal*, Vol. 71, No. 7, pp.647–659.
- Tian, T. and Hua, L. (2020) 'Research on sculpture art based on 3D printing technology', *Journal of Physics: Conference Series*, Vol. 1533, No. 2, p.022030.
- Wang, B., Kang, H., Sun, G. and Li, J. (2024) 'Efficient traffic-based IoT device identification using a feature selection approach with Lévy flight-based sine chaotic sub-swarm binary honey badger algorithm', *Applied Soft Computing*, Vol. 155, p.111455.

- Yu, X., Liu, Y. and Liu, Y. (2024) 'Optimization of WSN localization algorithm based on improved multi-strategy seagull algorithm', *Telecommunication Systems*, Vol. 86, No. 3, pp.547–558.
- Zhang, K. and Shen, Y. (2024) 'Interface capturing schemes based on sigmoid functions', *Computers and Fluids*, Vol. 280, pp.106352–106352.
- Zhao, Z., Guo, S., Han, L., Wu, L., Zhang, Y. and Yan, B. (2024) 'Altruistic seagull optimization algorithm enables selection of radiomic features for predicting benign and malignant pulmonary nodules', *Computers in Biology and Medicine*, Vol. 180, p.108996.
- Zhen, W., Dong, Z., Asghar, H.A., Yi, C., Huiling, C. and Guoxi, L. (2024) 'Improved Latin hypercube sampling initialization-based whale optimization algorithm for COVID-19 X-ray multi-threshold image segmentation', *Scientific Reports*, Vol. 14, No. 1, pp.13239–13239.
- Zhou, Y., Lin, Q., Wang, C., Guo, J., Yan, J. and Hong, J. (2024) 'Material stiffness optimization for homogenizing contact stress distribution based on particle swarm optimization using elite opposition-based learning mutation', *Mechanics of Advanced Materials and Structures*, Vol. 31, No. 28, pp.10033–10045.